Available online at www.sciencedirect.com
SCIENCE DIRECT®
PERGAMON
Annals of Nuclear Energy 30 (2003) 831–851
annals of NUCLEAR ENERGY
www.elsevier.com/locate/anucene

Computer simulation of corrosion product activity in primary coolants of a typical PWR under flow rate transients and linearly accelerating corrosion

Nasir M. Mirza[a,c,*], Muhammad Rafique[a], Muhammad Javed Hyder[b], Sikander M. Mirza[a]

[a]*Department of Physics & Applied Mathematics, Pakistan Institute of Engineering & Applied Sciences, Post Office Nilore, Islamabad 45650, Pakistan*
[b]*Department of Mechanical Engineering, Pakistan Institute of Engineering & Applied Sciences, Post Office Nilore, Islamabad 45650, Pakistan*
[c]*Center for Simulation Physics, University of Georgia, Athens, GA, 30602-2451, USA*

Received 1 July 2002; accepted 30 November 2002

Abstract

Computer simulation of behavior of coolant activation due to corrosion products have been investigated in a typical pressurized water reactor (PWR) under flow rate perturbations for linearly accelerating corrosion. The computer program CPAIR-P (Deeba et al., 1999) has been modified to accommodate for time dependent corrosion. Results for ^{24}Na, ^{56}Mn, ^{59}Fe, ^{60}Co and ^{99}Mo show that the specific activity in primary loop approaches equilibrium value under normal operating conditions fairly rapidly. During reactor operation, predominant corrosion product activity is due to ^{56}Mn and after shutdown cobalt activity dominates. These simulations suggest that the effect of flow rate perturbations on specific activity in the form of a depression in the activity curve can be smeared by a linearly rising corrosion. Such a dip can only be seen in activity when corrosion rate approaches to an equilibrium value well before the initiation of the transient. The time period to reach minimum coolant activity during transient is a function of the slope of flow rate perturbation parameter, $g(t)$. The new saturation value for activity depends on changes in flow rate (Δw) and equilibrium value (C_s) for the corrosion rate. For linearly accelerated corrosion and a pump coastdown condition, the activity does not show an initial drop when flow starts decreasing. It monotonically rises and

* Corresponding author. Fax: +92-51-9223727.
E-mail address: nasirmm@yahoo.com (N. M. Mirza).

doi:10.1016/S0306-4549(02)00142-1

follows the slope of corrosion rate. If the slope is greater than 9×10^{-6} μg/s^2, then the activity crosses the normal saturation value of 0.22 μCi/cm^3 before the reactor scram occurs. These results also indicate that the pump coastdown does produce a coolant activity spike before the reactor scram; however it can only be observed when the corrosion acceleration is fast.

Keywords: Computer modeling and simulation; Corrosion products; Flow rate transients in pressurized water reactors (PWRs); Corrosion rate

1. Introduction

Activated corrosion products in the primary coolant due to their long life and sizeable radioactivity can prohibit access to primary pumps, valves and its vicinity. The buildup of activity in the circulating coolant, on the coolant piping inner surfaces and on the core surfaces does pose problems to the reactor operation and maintenance in terms of accessibility demands. On one hand these problems are closely linked with the coolant purification, use of filters & corrosion inhibitors and on the other hand these are related to any rise in coolant temperatures, change in flow rates and perturbations in neutron flux (Mirza et al., 1989, 1991; Jaeger, 1970).

Various studies have shown that water becomes very corrosive at the high temperatures and pressures. The decomposition of water by radiation increases its corrosive nature. The corrosion products may originate as soluble and insoluble oxides, or in other particulate forms. The rate of corrosion in the reactor primary system keeps on increasing as the time of reactor operation at full power increases (Glasstone and Sesonske, 1981; Fontana, 1987; Hirschberg et al., 1999; Varga et al., 2001).

In pressurized water reactors (PWRs) the corrosion product activity is primarily due to short-lived ^{56}Mn and ^{24}Na. Nearly all the long-lived activity in the coolant is due to iron, molybdenum and cobalt with most significant radionuclides as ^{59}Fe, ^{99}Mo and ^{60}Co. Various nuclear properties of these nuclides are shown as Table 1

Table 1
Activation products and their reaction properties

Corrosion products	Reaction and neutron energy	Activation cross- section and half-life	λ-ray energy
^{24}Na	^{27}Al(n,α)^{24}Na	6×10^{-4} *b*	4.1
	(E_n > 11.6 MeV)	(15.4 h)	
	^{23}Na(n, λ)^{24}Na	0.53*b*	
	(E_n is thermal)	(15.4 h)	
^{56}Mn	^{55}Mn(n, λ)^{56}Mn	13.4*b*	2.13 (15%)
	(E_n is thermal)	(2.58h)	1.81 (24%)
^{59}Fe	^{58}Fe(n, λ)^{59}Fe	0.9*b*	1.17 (99.9%)
	(E_n is thermal)	45.1h	1.33 (99.9%)
^{60}Co	^{59}Co(n, λ) ^{60}Co	20.*b*	1.173 (99.9%)
		(5.3years)	1.332 (99.9%)
^{99}Mo	^{98}Mo(n, λ) ^{99}Mo	0.45*b*	0.78 (8%)
	E_n > 3.1 MeV	(67.0h)	0.74 (8%)

(Jaeger, 1970). The ^{55}Mn has an activation cross-section of 13.4b for the thermal neutrons to produce ^{56}Mn. The neutron activation of structural ^{27}Al and activation of ^{23}Na from salt impurities in water can produce ^{24}Na. The use of high-purity water, demineralization of water and the presence of filters keep the amount of dissolved salts to less than 0.05 ppm (Jaeger, 1970). It was seen for low powered nuclear plants, having large aluminum fraction in the system, the coolant activity due to Na-24 remained comparable to N-16 activity (Mirza et al., 1989, 1991). It was also shown in subsequent experimental studies that the effect of sodium salt as an impurity in coolant remains small as compared to ^{24}Na resulting from aluminum activation (Mirza et al., 1997a). However, the half lives of all corrosion products remains more than 2 h. Therefore, the primary coolant will always retain activity for several hours even after the reactor shutdown and any transient condition during operation can further increase the coolant activity.

We have to be cautious when the reactor coolant corrosion product experimental data are evaluated. Problems in withdrawing representative samples from PWR primary coolant through long sampling lines are well known in experimental studies. It has been suggested that measured concentrations of some corrosion products (e.g., soluble Co-60, Co-58 and Mn-54) are strongly dependent on sampling flow rate and born concentration (Kang and Sejvar, 1985; Polley and Anderson, 1989).

The turbulent flow of coolant in primary coolant loop keeps on depositing activated nuclides as it passes through the flow channels of the primary coolant loop. These deposits of dissolved and suspended radionuclides on the scale of cooling system inner surfaces do pose maintenance issues. Chemical procedures to separate the corrosion products in primary coolants of PWRs after shutdown were carried out by Raymond et al to find concentrations of target and active nuclides. They showed that detection limits are between 0.05 and 0.3 mg/l for undissolved species and for ions these are in the range of 0.03–0.14 mg/l for sample volumes of 0.5 l (Raymond et al., 1987). Recently Hirschberg and his colleagues have also experimentally studied accumulation of radioactive corrosion products on steel surfaces of VVER type nuclear reactors. These were laboratory scale studies for Co-60 buildup on steel surfaces (Hirschberg et al., 1999; Varga et al., 2001).

Operating parameters of the reactor also strongly affect the types of radionuclides formed, the levels of saturation activity reached and the rates at which the saturation is reached. These include the composition of the materials in contact with the coolant, amount and the types of the impurities present in the coolant, reactor power, residence time of coolant in core, temperatures and pressure, coolant flow rates, corrosion rates, filter efficiency and deposition rates of radioactive elements in coolant.

During the past decade many studies were conducted on coolant activation with specific interest to find effects of flow rate and power perturbation on dose rate in medium flux research reactors (Mirza et al., 1989, 1991). Calculations of coolant activation were also done for low flux natural convection based systems (Mirza et al., 1993a,b). Experimental measurements of sodium-24 activity in low power research reactors yielded that majority of Na-24 comes from neutron activation of Al-27 and its subsequent mixing in coolant and it is second important contributor to the total dose after N-16 in coolant activity. (Mirza et al., 1997a).

During the past 10 years, a series of studies were done on coolant activation in reactors and effects of flow rate and power perturbations remained in focus. It was seen in simulations of low and high flux systems that transients under reactivity and loss of flow do lead to peaking of neutron flux in reactor and production of activity in coolant (Iqbal et al., 1996, 1998; Mirza et al., 1998). These strongly affect the coolant activity and corrosion rate. Void coefficient, Doppler coefficient and temperature of moderator showed significant effects on power peaking in a non-uniform manner within the core. It also led to the necessity of performing detailed space and time calculations of flux for conditions (Khan et al., 1999). Sensitivity analysis of reactivity insertion limits with respect to safety parameters in typical Material Test Reactors showed that neutron flux peaking and clad melting conditions are dictated by void coefficients, transient type and their rates (Nasir et al., 1999).

Modeling of corrosion products activity in primary coolants of PWRs under flow rate perturbations were also done to investigate effects due to flow coast down and linear decrement of flow (Mirza et al., 1997b). A computer code CPAIR was developed in FORTRAN-77 to calculate specific activity due to ^{24}Na, ^{56}Mn, ^{59}Fe, ^{60}Co and ^{99}Mo in primary water of light water reactors. It was shown that minimum value of coolant activity depends strongly on the slope of linear decrement of flow rate. The program was further improved to incorporate the effect of power perturbations on corrosion product activity in coolants of a PWR (Deeba et al., 1999). The computer code was modified as CPAIR-P and effects of fast and slow transients were studied on dose rates due to corrosion activity in coolant All these studies assumed a constant and uniform corrosion rate during and after transients. However, the corrosion rate does increase slowly with plant aging; it also increases with temperature and pressure. The rate of increase of corrosion depends on integrated effect of neutron flux, time of reactor operation and reactor temperatures (Fontana, 1987; Glasstone and Sesonske, 1981).

This work aims at simulating the behavior of corrosion product activity in a typical PWR when corrosion rate is changing linearly in primary circuit. These changes are superimposed on flow rate perturbations. The computer program CPAIR-P (Mirza et al., 1998; Deeba et al., 1999) was modified to incorporate both the linearly changing corrosion rates and flow rate perturbations. First, we compared the activity for fixed corrosion rate under different flow rate transients in a PWR. Then, both accelerating corrosion rates and different types of flow rate perturbations were introduced and the behavior of corrosion product activity in primary coolants was studied. We have tested the program against experimental results for Trojan plant spiking activities in primary coolant during shutdown process. Results for fast and slow corrosion acceleration and flow rate perturbations are presented here.

2. Mathematical model

The time dependent concentration comes from a balance between the rate of production of radioactive nuclei and the rate at which they are lost as a result of

purification, deposition on surfaces, leakage and radioactive decay. All these possible pathways leading to the productions and losses of corrosion product are shown in Fig. 1. We have assumed a uniform time dependent corrosion in the coolant circuit and have ignored the space distribution effects. The deposition of the activity on surfaces in contact with the cooling water is proportional to the concentration of the corrosion products in water. Ion exchangers and filters are assumed to remove impurities in proportion to their concentration in the coolant.

The concentration of target nuclides in the primary coolant water, on the inner walls of the piping and on the core surfaces have been denoted by N_w, N_p and N_c respectively in atoms/cm^3. Also the concentrations of the activated nuclides in primary water, on the piping and on the core have been represented by n_w, n_p and n_c respectively, in atoms/cm^3. Then the rate of change of active material concentration in primary coolant is (Mirza et al., 1997b; Deeba, et al., 1999):

$$\frac{dn_w}{dt} = \sigma\phi_\varepsilon N_w - \left\{\sum_j \frac{\varepsilon_j Q_j g(t)}{V_w} + \sum_k \frac{l_k g(t)}{V_w} + \lambda\right\} n_w + \frac{K_p g(t)}{V_w} n_p + \frac{K_c g(t)}{V_w} n_c \qquad (1)$$

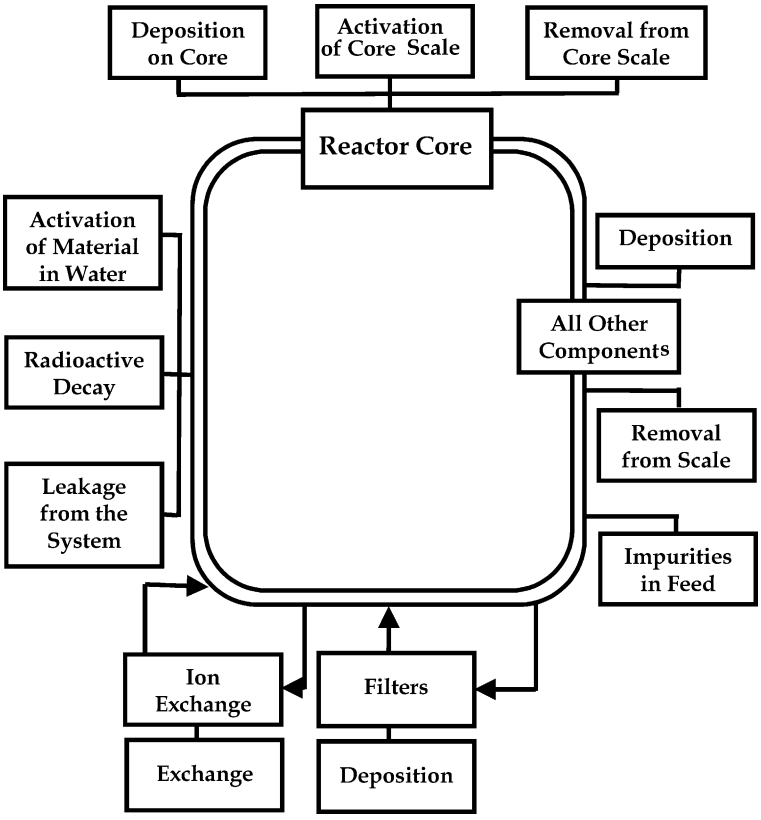

Fig. 1. Various paths leading to the production and loss of corrosion products in primary coolant circuit of a typical PWR.

where σ is the group constant for the production of isotope from target nuclide; ϕ_ε is the effective group flux (neutrons per cm^2 per s); N_w is the target nuclide concentration in water (in atoms per cm^3). The sum over j for $\varepsilon_j Q_j$ is given as following:

$$\sum_j \varepsilon_j Q_j = \varepsilon_I Q_I + \varepsilon_p Q_p + \varepsilon_c Q_c + \varepsilon_F Q_F \tag{2}$$

where the quantities $\varepsilon_I Q_I$, $\varepsilon_p Q_p$, $\varepsilon_c Q_c$ and $\varepsilon_F Q_F$ are removal rates due to ion exchanger, deposition on pipes, deposition on core surfaces and removal by filters, respectively. The term l_k is the rate at which primary coolant loop loses water from its k'th leak (in cm^3 per second); K_p and K_c are rates at which isotopes are removed from the scale on piping (cm^3 per second) and from the core (in cm^3 per second) respectively. For a typical PWR the measured values of these removal rates are shown in Table 2. The first term represents the production of radioactive isotopes. The second term is the rate at which the active nuclides are lost as a result of purification by the ion-exchanger and filters, deposition on the piping and core and decay. The third and fourth terms are the rates at which the activity is re-introduced into the coolant by erosion from scale on piping and the core. To include any flow rate perturbation we define a parameter $g(t)$:

$$g(t) = w(t)/w_0 \tag{3}$$

where w_0 is the steady state flow rate under normal operations and $w(t)$ is the time dependent flow rate. The averaged neutron flux for a given energy group is also affected by the flow rate changes as

$$\phi_\varepsilon = \left\{\frac{1-\exp(-\lambda T_c)}{1-\exp(-\lambda T_L)}\right\}\phi_0 \tag{4}$$

The values of decay constant (λ) for each isotope of interest are provided in Table 1. The group flux ϕ_0 is averaged over the geometry of the core and have been estimated using LEOPARD (Barry, 1963) and ODMUG (Thomas and Edlund, 1980) in the program CPAIR-P. The time T_c and T_L are the core residence time and

Table 2
Experimental values of exchange rates in a typical PWR[a]

Rate type	Value
Deposition on core ($\varepsilon_c Q_c$):	80.0 cm^3 per second
Deposition on piping ($\varepsilon_p Q_p$):	13.7 cm^3 per second
Ion-exchanger removal ($\varepsilon_I Q_I$):	500–781 cm^3 per second
Re-solution ratio for core (K_c):	40.0 cm^3 per second
Re-solution ratio for piping (K_p):	6.9 cm^3 per second
Volume of primary coolant (V_w):	1.37×10^7 cm^3
Volume of scale on core (V_c):	9.08×10^6 cm^3
Volume of scale on piping (V_p):	1.37×10^6 cm^3
Total corrosion surface (S):	1.01×10^8 cm^2
Average corrosion rate (C_o):	2.4×10^{-13} gm per cm^2 per second

[a] References: Jaeger, 1970; Glasstone and Sesonske, 1981.

loop time (required to complete the primary loop once) respectively. The core residence time is

$$T_c = \frac{H\rho A}{w(t)} \tag{5}$$

where H is the core height; A is the flow cross-sectional area in cm^2; ρ is the coolant density at operating temperatures and $w(t)$ is the time dependent flow rate (g per second). The loop time is approximated as $L_p T_c/H$ for the complete loop length L_p.

The rate of build-up of target nuclide concentration in coolant water can be written as

$$\frac{dN_w}{dt} = -\left\{\sum_j \frac{\varepsilon_j Q_j g(t)}{V_w} + \sum_k \frac{l_k g(t)}{V_w} + \sigma\phi_\varepsilon\right\} N_w + \frac{K_p g(t)}{V_w} N_p + \frac{K_c g(t)}{V_w} N_c + S_w \tag{6a}$$

$$S_w = \frac{C(t) S}{V_w} \frac{N_0}{A} f_n f_s \tag{6b}$$

where, N_p is concentration of target nuclide on the piping; N_c is concentration of target on the core, and S_w is the source term for corrosion. The $C(t)$ is the time dependent corrosion rate (gram per cm^2 per s); S is the area of system exposed to coolant for corrosion; N_0 is Avogadro's number (6.023×10^{23} atoms per g-mole) and A is the atomic weight of the target nuclide (gram). Here, f_n and f_s are abundances of target nuclide and chemical element in the system respectively.

The impurity removal by ion-exchanger, core deposition and leakage are directly related to the flow rate. Also, the rate of re-entry from scales is directly proportional to the primary coolant flow rate. Therefore the rate of activity build-up on the core scale is given by

$$\frac{dn_c}{dt} = \sigma\phi_0 N_c + \frac{\varepsilon_c Q_c g(t)}{V_c} n_w - \left\{\frac{K_c g(t)}{V_c} + \lambda\right\} n_c \tag{7}$$

where, V_c is volume of the scale on the core (cm^3) and ϕ_0 is thermal neutron flux average over the geometry of the core (neutrons/cm^2−s).

The rate of buildup of target nuclide concentration on the core scale (N_c) is given by the following equation:

$$\frac{dN_c}{dt} = \frac{\varepsilon_c Q_c g(t)}{V_c} N_w - \left\{\frac{K_c g(t)}{V_c} + \sigma\phi_0\right\} N_c \tag{8}$$

The rate of deposition of active material on the piping scaling (n_p) can be obtained from following balance:

$$\frac{dn_p}{dt} = \frac{\varepsilon_p Q_p g(t)}{V_p} n_w - \left\{\frac{K_p g(t)}{V_p} + \lambda\right\} n_p \tag{9}$$

where V_p is the volume of scale on the piping (cm^3). Then the rate of change of target nuclide on piping walls (N_p) is

$$\frac{dN_p}{dt} = \frac{\varepsilon_p Q_p g(t)}{V_p} N_w - \frac{K_p g(t)}{V_p} N_p \tag{10}$$

Based on the above system of Eqs. (1)–(10), the computer program CPAIR-P (Corrosion Product Activity In Reactors) (Mirza et al., 1997b) was modified for this work to include the effect of both accelerating corrosion rate and flow rate perturbations as a function of time. The modified CPAIR-P program is written in FORTRAN-77 for Personal Computers. It now calculates the corrosion product activity as a function of reactor operation time under both time dependent corrosion and flow rate perturbations. Overall computational algorithm is illustrated in the form of a flow chart (Fig. 2). After initialization, it calculates group constants using core design parameters (Table 3) in LEOPARD (Barry, 1963) code. The LEOPARD program is a zero-dimensional unit cell computer code with 54 fast and 172 thermal energy groups. An early data set is used in the cross section library. In this work equivalent cells of a typical PWR (Glasstone and Sesonske, 1981) have been employed to generate group constants for fuel cells and water holes. These cell-averaged group constants are then employed in the one-dimensional multigroup diffusion theory based ODMUG (Thomas and Edlund, 1980) code. Using ODMUG, the group fluxes as a function of position in the reactor are calculated. These group fluxes are subsequently averaged over the core. Both LEOPARD and ODMUG are treated as subroutines of the CPAIR-P program. Then, in next step, Eqs. (1)–(10) are used to find the activity values due to corrosion products in primary coolant, on piping, and on core surface. The set of simultaneous differential equations are solved using fourth-order Runge–Kutta method. Program has three loops to study the corrosion rate changes, flow rate perturbations and activity due to each isotope (Fig. 2) with an overall loop over time steps.

3. Simulation results

A typical PWR (Glasstone and Sesonske, 1981) is considered with initial concentration of the impurities taken to be zero. Experimental data has been employed in the analysis for the fractional exchange rates ($\varepsilon_j Q_j / V_q$) and re-solution rates (K_j / V_q). The values have been taken from Jaeger (1970) and are shown in Table 2. The design data values for a typical PWR are shown as Table 3 (Glasstone and Sesonske, 1981). The core averaged group fluxes have been computed using LEOPARD and ODMUG codes. The plant surface area of 10^8 cm^2 is exposed to the primary coolant for corrosion and an equilibrium corrosion rate of 2.4×10^{-13}g/cm^2 s (Jaeger, 1970) exists after a year of reactor operation. It has primary coolant volume of $1.3\times10^7 cm^3$. We assumed parameters $f_n = 1.0$ and $f_s = 0.5$ for Mn-56 to be on conservative side. Then the corrosion rate of 25 μ g/s has been used as normal equilibrium rate in our subsequent studies.

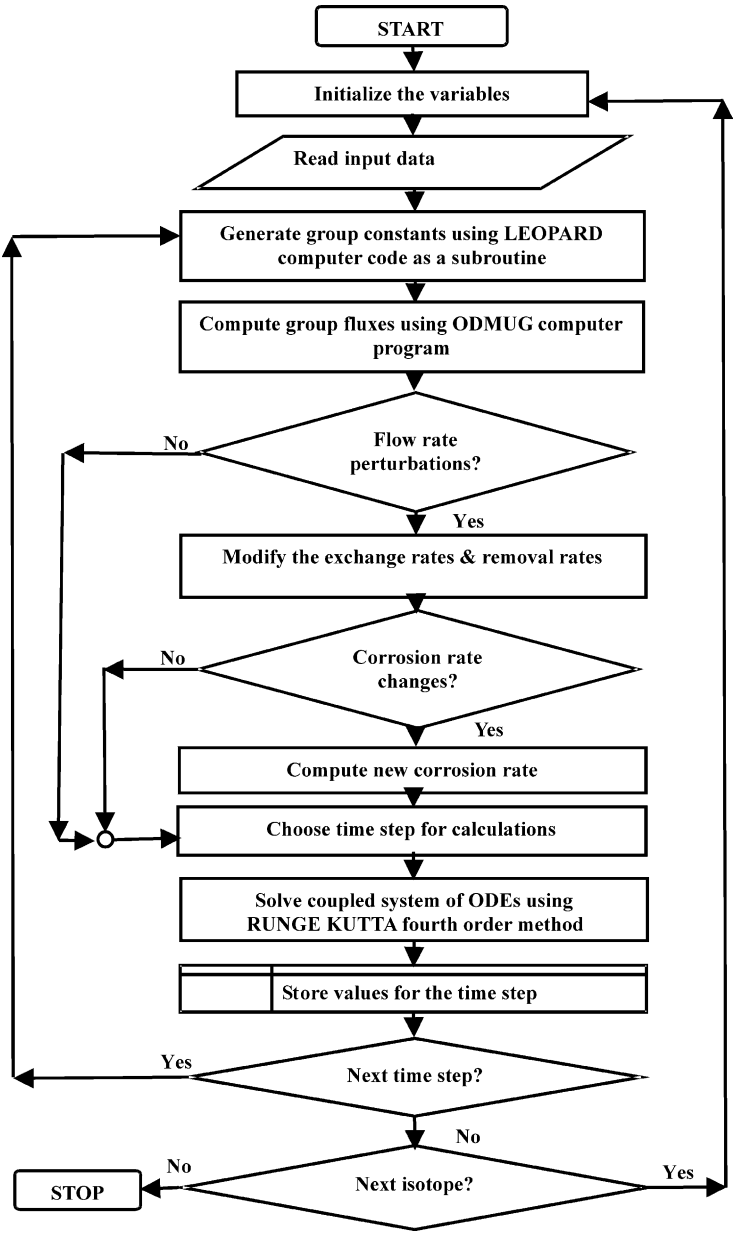

Fig. 2. Flow chart of CPAIR-P (Corrosion Product Activity in Reactors—Version P) computer program.

The simulations are started at time $t=0$, when the reactor is considered to be operating at full power without any impurity. The purification rate due to an ion-exchanger, $\varepsilon_I Q_I$, must be large enough to regard deposition, re-solution and leakage as second-order effects. Therefore, using an approach by Mirza et al. (1997a,b) an

Table 3
Typical design specifications of a PWR

Parameter	Value
Specific power [MW(th)/kg U]	33
Power density [MW(th)/m^3]	102
Core height (m)	4.17
Core diameter (m)	3.37
Assemblies	194
Rods per assembly	264
Fuel type	UO_2
Clad type	Zircoloy
Lattice pitch (mm)	12.6
Fuel rod outer diameter (mm)	9.5
Average enrichment (^{w}%)	3.0
Flow rate (Mg/s)	18.3
Linear heat rate (kW/m^2)	17.5
Coolant pressure (MPa)	15.5
Inlet coolant temperature (°C)	293
Outlet coolant temperature (°C)	329

optimum removal rate of activity by the ion-exchanger was determined at a constant corrosion rate (25 μg/s). It was found that saturation value of coolant activity remains fixed when $\varepsilon_I Q_I$ is more than 400 cm^3 per second. Thus a removal rate of 600 cm^3 per second was selected for which the saturation value is sufficiently low ($\sim$0.22 μCi/cm^3).

Five corrosion products (^{56}Mn, ^{24}Na, ^{59}Fe, ^{60}Co and ^{99}Mo) were considered in this study. The isotope ^{56}Mn remained the largest contributor to the total activity (Fig. 3) during reactor operation at full power. However, cobalt isotopes dominate the coolant activity after shutdown. Its activity is about 36% of the total corrosion product activity in the PWR whereas other isotopes including ^{24}Na, ^{59}Fe, ^{99}Mo and ^{60}Co contribute about 23.4%, 29.6%, 9.5% and 1.4% respectively. The activity due to ^{56}Mn saturates at about 150 h after start of the reactor. Its saturation value is 0.22 μCi/cm^3 and it makes the primary coolant as a 0.663MCi source within 150–230 h of reactor operation at full power. These are close to the values already reported by Mandler et al. (1985) and Volleque (1990) in their source term measurements.

3.1. Constant corrosion rate and flow rate perturbations

Flow rate perturbations in a PWR can occur due some variation in the cross sectional area of the flow path or due to a primary pump speed variation. These perturbations subsequently affect temperatures, neutron flux in the core, corrosion production terms and loss terms. The load-following system then may try to adjust the flow rates in the reactor; however, if it cannot do so then the reactor will scram. In this work, flow perturbations are introduced during the steady state operation of the reactor when corrosion products activity has reached its saturation value. Then

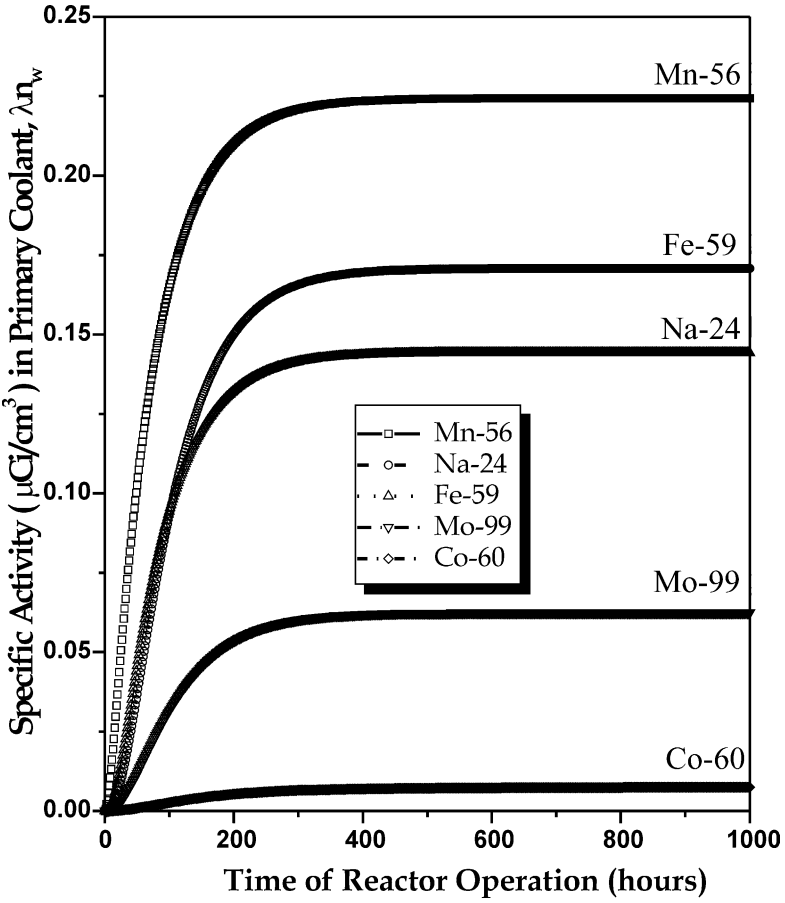

Fig. 3. Specific activity of various corrosion products as a function of reactor operation time under normal conditions and constant corrosion rate.

effect on coolant corrosion product activity is observed using the CPAIR-P program. First we have computed the activity when a constant corrosion rate (25 μg/s) is present in the system.

A linear decrease in flow rate is introduced (at $t = 500$ h) for the reactor operating at full power under steady state conditions. Corrosion products have reached saturation values in the primary coolant and the reactor is not allowed to undergo a scram during the transient. This linear decrease in the flow can be described by a parameter $g(t)$:

$$\begin{aligned} g(t) &= 1.0, \quad t < t_{\text{in}} \\ &= 1.0 - \alpha(t_{\text{in}} - t), \quad t_{\text{in}} < t < t_{\max} \\ &= w_2/w_0, \quad t > t_{\max} \end{aligned} \tag{11}$$

where α is the slope of linear flow rate decrement and t_{in} is the time at which the disturbance in the mass flow rate is initiated. After time t_{max} the flow rate achieves a lower value of w_2 as compared to w_0.

In the first part of the study, the above parameter $g(t)$ is introduced as a perturbation while the corrosion rate is kept constant. The flow rate is introduced at $t_0 = 500$ h for various Δw changes for a period of 50 h. Resulting specific activity from the CPAIR-P code as a function of time is shown in Fig. 4a and b. As the flow rate decrease to 10% of its rated value, the corrosion product specific activity first decreases monotonically and then it starts increasing again to a new saturation value (see curve B in Fig. 4b). As soon as the flow rate reaches the lower values of $0.9w_{0,}$ the activity attains a new saturation value of 0.23 $\mu Ci/cm^3$. This effect is pronounced further when we test the plant for even lower values of flow rate as shown in Fig. 4b (curves C–E).

As the flow rate decreases dictated by the balance Eq. (11), both the time periods T_c and T_L increase and this translates into an increase in the exposure of corrosion products to the neutron fluxes in the core region. Eqs. (6)–(10) show that terms $\left(K_p g(t)/V_w\right)N_p$ and $(K_c g(t)/V_w)N_c$ are directly related to mass flow rate of the coolant in the primary circuit. It should be kept in view that K_c and K_p are the rates at which material is removed from scale on core and piping respectively. Also, the factors, $\sum \varepsilon_j Q_j$, $\sum l_k$ and effective neutron flux are directly related to the flow rate perturbations. Moreover, when primary coolant flow rate decreases the equilibrium neutron temperature rises and affects the production of corrosion product activity. In these flow rate perturbation hypothetical tests, we have forced the reactor to keep operating at full power. Therefore, an initial decrease in flow rate causes a quick increase in the loss rates that remain dominant initially and cause a dip in the coolant activity. When flow rate becomes constant to a new low value, the gain terms in the balance take over and the activity eventually attains a new higher value due to an increase in the effective production rate of corrosion products.

In second part, the slope (α) of the linear decrement in flow rate is changed from 0.01 to 0.001 for a fixed change in mass flow rate (10% of w_0). Simulation results are shown in Fig. 5. It illustrates the specific activity for Mn-56 in the coolant. In this scenario, the time taken to reach a minimum activity also changes. This time period is about 10 h for a slope value (α) of 0.01. It gets larger as the slope value is varied to smaller values. So, the time period to reach minimum coolant activity during transient is a function of the slope of flow rate perturbation parameter, $g(t)$, while the corrosion rate is fixed.

3.2. Linear acceleration of corrosion

Slow and fast linear acceleration have been studied using following model for time dependent corrosion rate $C(t)$:

$$\begin{aligned} C(t) &= 0, \quad t < a \\ &= \frac{\Delta C}{\Delta t}(t - t_0), \quad a \leqslant t \leqslant b \\ &= C_s, \quad t > b \end{aligned} \tag{12}$$

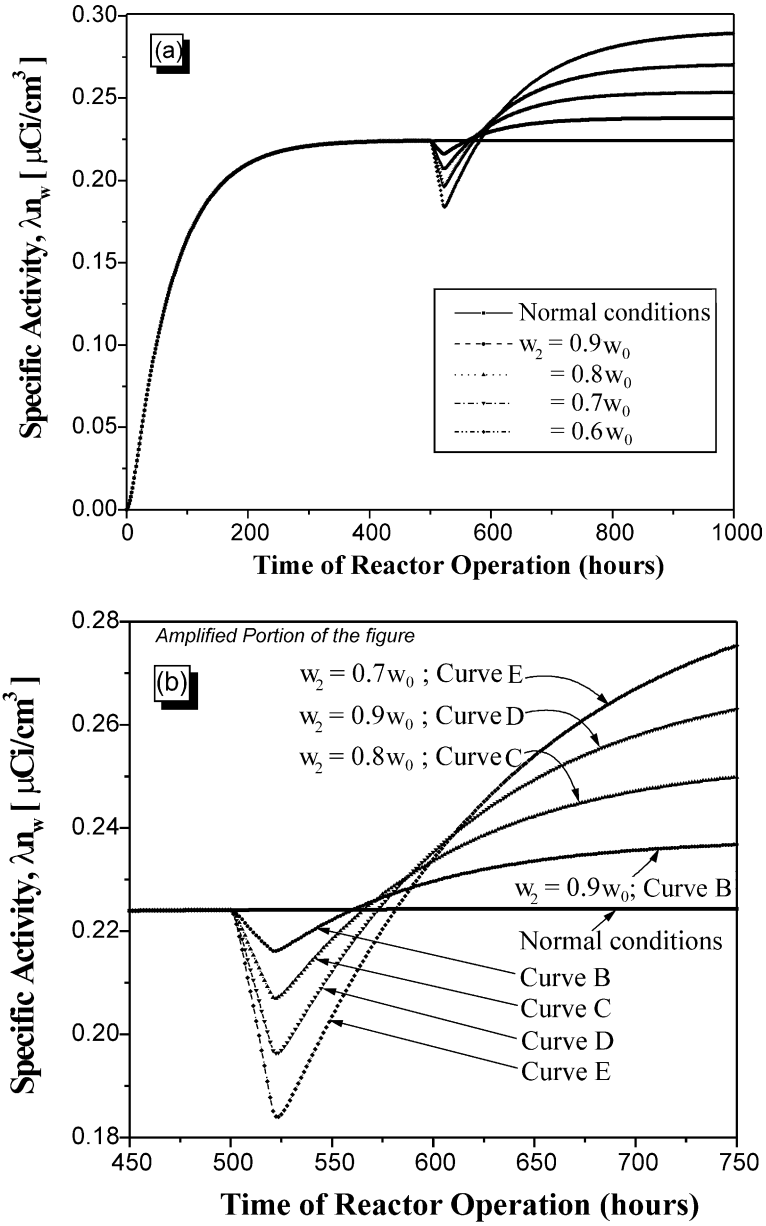

Fig. 4. (a) Specific activity due to Mn-56 in primary coolant of a PWR under linear flow rate perturbation for various Δw and constant slope values. The corrosion rate is assumed to be constant (25 μg/s) and uniform. (b) Amplified portion of the curves for time period: 450 h < time < 750 h.

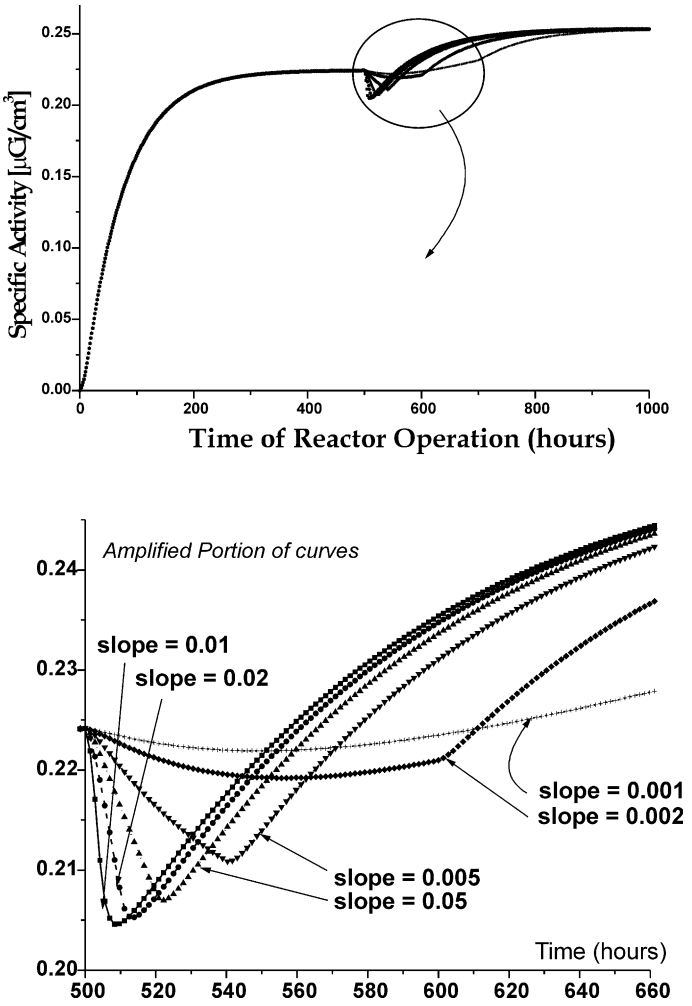

Fig. 5. Specific activity due to Mn-56 in primary coolant under linear flow rate perturbation, initiated at $t = 500$ h, for fixed Δw at various slope values. Constant corrosion rate (25 μg/s) is assumed.

where $\Delta C/\Delta t$ is a non-zero positive constant slope of corrosion rate in the time domain $[a,b]$ and C_s is the equilibrium value of the rate after time b. We assume corrosion-free time period of about 50 h after the startup. Fig. 6a shows the normalized corrosion rate versus time for an equilibrium value (C_s) using above model. When we introduce such a time dependent corrosion rate along with a flow rate perturbation, the resultant specific activity for Mn-56 is shown in Fig. 6b. The activity follows the corrosion rate curve and its slope is in accordance with $\Delta C/\Delta t$. The linear flow rate introduced at $t_0 = 500$ h, does produce same depression in the activity and the height of the activity depression keeps on decreasing as the acceleration in corrosion gets smaller and smaller (Fig. 6b). It becomes less than 5% of

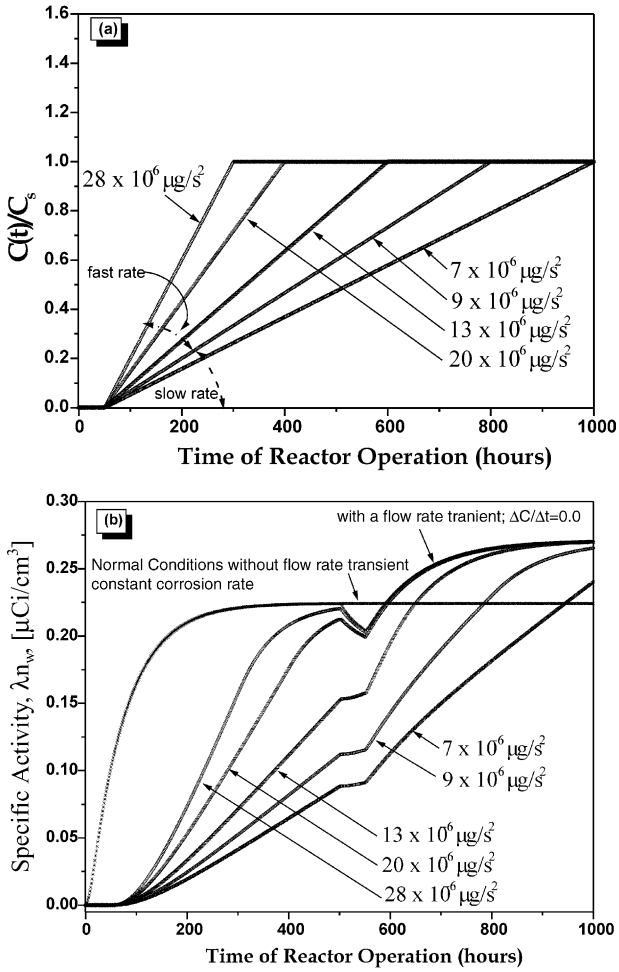

Fig. 6. (a) Normalized corrosion rate as a function of reactor operation time for different values of $\Delta C/\Delta t$ and fixed equilibrium value of 25 μg/s. (b) Specific activity due to Mn-56 in primary coolant of a PWR under flow rate transient ($\Delta w = 0.3 w_0$) initiated at $t = 500$ h for various linearly rising corrosion rates shown in part (a).

normal saturation activity (0.22 μCi/cm^3) for $\Delta C/\Delta t = 7\times10^{-6}$ μg/s^2. The activity in all cases eventually approaches to a new saturation value. The time taken to reach or cross the normal saturation value of 0.22 μCi/cm^3 is relatively high. It increases with a decrease in $\Delta C/\Delta t$ value as shown in Table 4. For a slow acceleration ($\Delta C/\Delta t \leqslant 10^{-5}$ μg/s^2), the time taken to cross the normal saturation value is about 915 h as compared to 230 h when a constant corrosion rate is used (Fig. 6b and Table 4). These results suggest that effect of flow rate perturbations on specific activity in the form of a dip in activity curve can be smeared by a linearly rising corrosion. Such a dip can only be seen in activity when corrosion rate satu-

Table 4
Time taken to reach normal saturation activity[a] as a function of $\Delta C/\Delta t$ for a fixed linear flow rate transient[b]

$\Delta C/\Delta t$ ($\mu g/s^2$)	Time taken (h)
0.0	230
28×10^{-6}	580
20×10^{-6}	631
$13\times10^{-6?}$	762
9×10^{-6}	915

[a] Normal saturation activity value = 0.22 $\mu Ci/cm^3$ for Mn-56.
[b] $\Delta w = 0.3 w_0$ initiated at $t = 500$ h for 50 h.

rates to a constant value well before the initiation of the transient. The new saturation value depends on changes in flow rate (Δw) and equilibrium for corrosion rate C_s.

In next part we studied the behavior of coolant activity by changing the slope of the corrosion rate ($\Delta C/\Delta t$) as well as C_s while the flow rate perturbation remained same ($\Delta w = 30\%$ of w_0, initiated at $t = 500$ h for a period of 50 h). The acceleration for corrosion is allowed to have different slopes and equilibrium values. The resulting activity due to Mn-56 in coolant is illustrated as Fig. 7. It is noticeable that the activity in the coolant attains new saturation value after the transient and this saturation value keeps on increasing with increase in equilibrium value (C_s). It implies that new saturation activity after a flow rate transient depends on both the equilibrium value of corrosion rate (C_s) and change in flow rate (Δw). However, the time taken to reach the saturation activity in coolant depends on the slope of corrosion rate.

To test the modified program against relatively clean experimental results, we have selected spiking of coolant activity reported during shutdown processes in typical PWRs (Bergmann and Roesmer, 1984). During the shutdown, the spiking activities were observed in several PWRs and a typical spiking data for Trojan Plants is shown as solid circles in Fig. 8 (Bergmann and Roesmer, 1984). The cobalt activity increases rapidly with the boron addition and when the coolant temperature is reduced to 300 °F. Another spike in activity occurs when hydrogen peroxide is added to the system as shown in figure. We have used the same shutdown sequence and related data to simulate the corrosion product activity using CPAIR-P program. We tested the constant corrosion rates and various accelerating corrosion rates in the system and it was found that results for rate of 7×10^{-6} $\mu g/s^2$ become close to the experimental data for spikes. We did allow the system to operated at full power for 1000 h to achieve equilibrium in these simulations. The computational results are also shown against the experimental data as Fig. 8. The program predicts a higher value of first spike resulting from the boron control and cooling of the system. This has been predicted around the same time period as measured in experiments. However, the second spike due to introduction of H_2O_2 is close to experimental results and subsequent decrease in activity is also predicted well by the

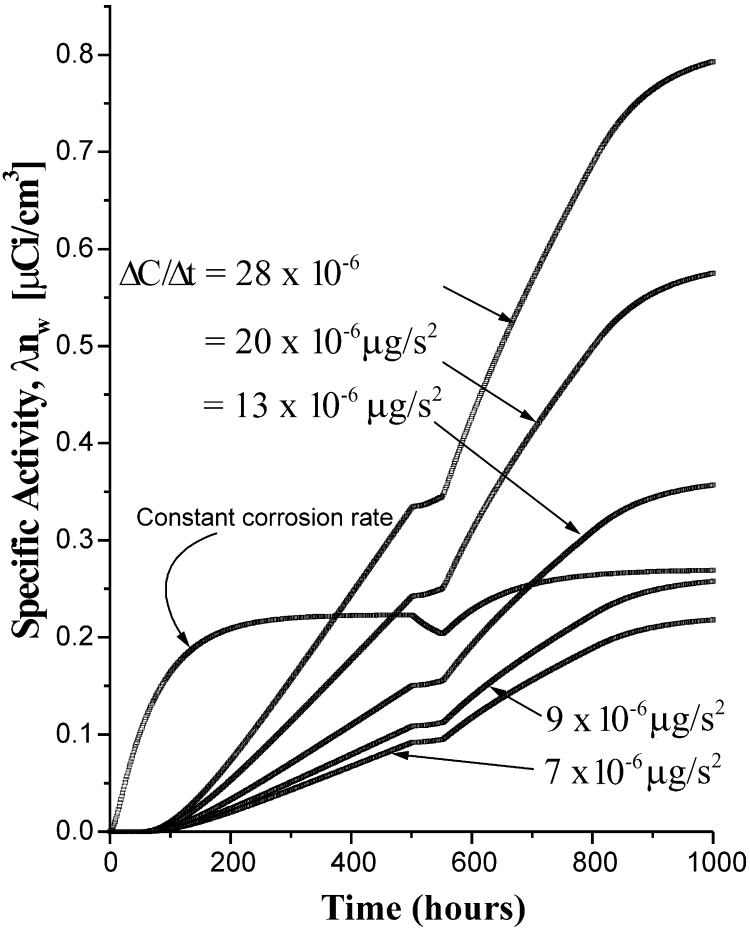

Fig. 7. Specific activity due to Mn-56 in primary coolant of a PWR under flow rate transient ($\Delta w = 0.3 w_0$) initiated at $t = 500$ h for various linearly rising corrosion rates with different slopes and equilibrium values.

program. This test, however, contained coupled effects of both power reduction and temperature changes in the system and does not contain feedback effects of flow rate perturbations on corrosion rates. In subsequent simulations we have treated only the flow rate perturbations while keeping the power fixed.

3.3. Pump coastdown model

The flow coast down due to decease in speed of a primary pump can be obtained by equating the frictional retarding force to the changes in the momentum of the fluid. The balance for a given average velocity (v) and fluid density (ρ) is given as (Lewis, 1977):

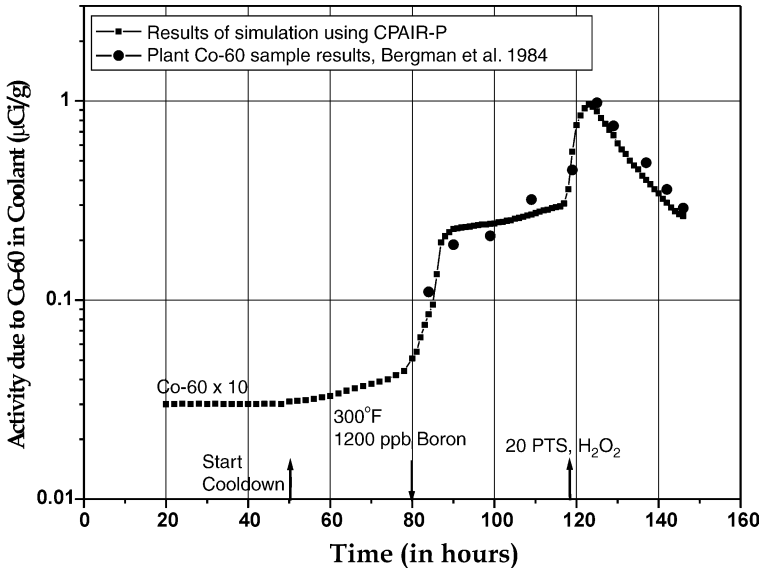

Fig. 8. Comparison of activity due to Co-60 in Trojan Plant's primary coolant during a shutdown sequence. The circles indicate plant measured data values and solid squares show the simulation results from CPAIR-P program.

$$\frac{L\rho}{g_c}\frac{dv}{dt} = -C_f\frac{\rho v^2}{2g_c} \tag{13}$$

where L is the total length of the loop and C_f is the total pressure loss coefficient for the loop. The solution in terms of flow rate is

$$w(t) = w_0/(1 + t/t_p) \tag{14}$$

The time t_p is flow half-time ($2L/C_f v_0$). An initial flow rate for steady state reactor operation is w_0 and $w(t)$ is flow rate at any time t. In this study, we considered t_p large enough so that the boiling crisis does not occur until after the reactor trip.

Using modified CPAIR-P, the pump coastdown is introduced in the primary coolant circuit of a PWR for a given t_p value. Then activity in coolant is estimated for both a constant corrosion rate and a linearly accelerating corrosion of the type discussed in Section 3.2. The results are shown in Fig. 9. For a constant corrosion rate, the flow coastdown is started at $t = 500$ h after the reactor startup. Decrease in flow rate causes an initial decline in the activity and slope of this decline depends on flow half-time (t_p). Then the activity in coolant starts rising and keeps on rising until the flow rate reaches 90% of the initial flow rate value and the reactor scrams. After scram, the average neutron flux becomes very low and the coolant activity follows it.

For a case of linearly accelerated corrosion rate with a pump coastdown, the coolant activity does not show an initial drop with flow decrement. It monotonically rises and follows the slope of corrosion rate. If the slope is greater than 9×10^{-6} μg/s^2, then activity crosses the normal saturation value of 0.22 μCi/cm^3 before the

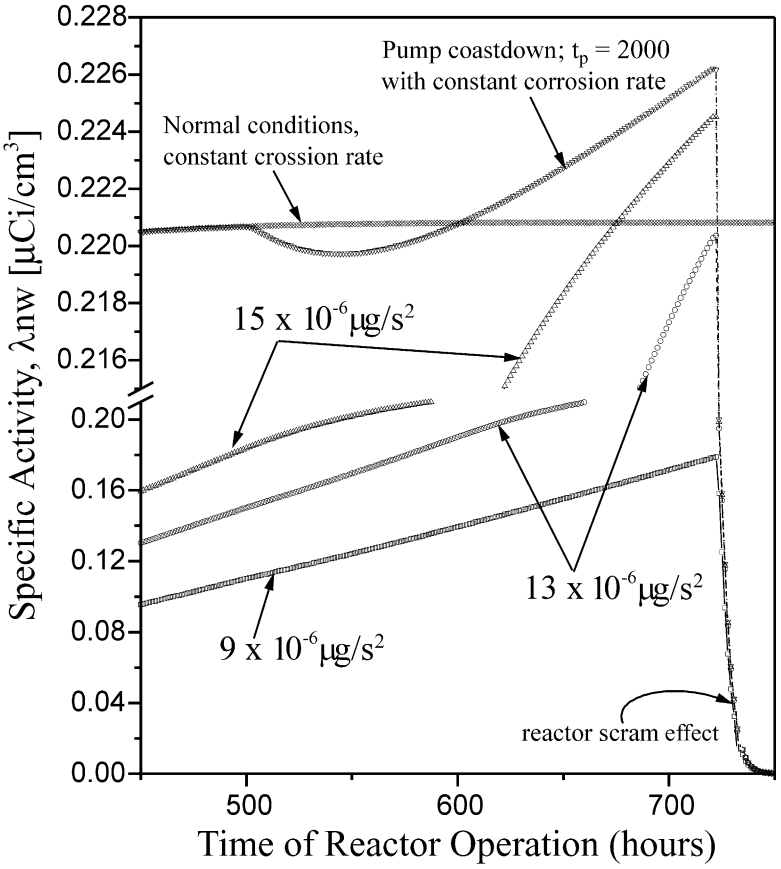

Fig. 9. Specific activity due to Mn-56 in primary coolant of a PWR under flow coastdown (t_p = 2000 h) initiated at t = 500 h for various linearly rising corrosion rates. Reactor was allowed to scram at 90% of its rated flow rate.

reactor scram occurs. These results indicate that pump coast down does produce a coolant activity spike before the reactor scram; however it can only be seen if the corrosion acceleration is fast (i.e., more that 10^{-5} μg/s^2).

4. Conclusions

For linearly accelerating corrosion, simulation of coolant activation due to corrosion products have been done in a typical PWR under flow rate perturbations. In the first part of the work, the computer program CPAIR-P (Deeba et al., 1999) has been modified to accommodate for a time dependent linear corrosion rate model. Results for ^{24}Na, ^{56}Mn, ^{59}Fe, ^{60}Co and ^{99}Mo show that the specific activity in primary loop approaches equilibrium value under normal operating conditions fairly rapidly. It was observed that the modified program predictions remain close to the

experimental results for corrosion product activity spikes during shutdown process. Then flow rate perturbations were simulated for different linearly accelerating corrosion and their effects on saturation activity were studied. For a linear decrease in flow rate and a constant corrosion rate, the coolant activity first decreases sharply from its saturated value and reaches a minimum value. Then it starts increasing and approaches to a new higher saturation value. The minimum value and the time taken to reach the minima are strong function of the slope of linear decrease in flow rate. When a linearly accelerating corrosion is introduced, the behavior of specific activity changes considerably. These simulations suggest that effect of flow rate perturbations on specific activity in the form of a dip in activity curve can be smeared by a linearly rising corrosion. Such a dip can only be seen in activity when corrosion rate saturates to a constant value well before the initiation of the transient. The new saturation value depends on both the changes in flow rate (Δw) and an equilibrium value for corrosion rate (C_s). For a pump coastdown ($t_p = 2000$ h), the activity does not show an initial drop when flow rate starts decreasing. It monotonically rises and follows the slope of corrosion rate. If the slope is greater than 9×10^{-6} μ/s^2, then activity crosses the saturation value of 0.22 $\mu Ci/cm^3$ before the reactor scram occurs. These results indicate that pump coastdown does produce a coolant activity spike before the reactor scram; however it can be observed when the corrosion acceleration is fast (i.e., more than 10^{-5} $\mu g/s^2$).

Acknowledgements

We are thankful to Dr. Abdullah Sadiq, Dr. Matiullah and Dr. Anwar Mirza for valuable discussions. Two of us (N.M.M. and M.R.) wish to thank the Ministry of Science and Technology, Pakistan for support by fellowships. The support of computational facilities at PIEAS and Center for Simulation Physics, UGA is also gratefully acknowledged.

References

Barry, R.F., 1963. LEOPARD: A Spectrum Dependent Non-Spatial Depletion Code for IBM-7094 (WCAP-3269-26). Westinghouse Electric Corporation.

Bergmann, C.A., Roesmer, J., 1984, March. Coolant chemistry effects on radioactivity at two pressurized water reactor plants (EPRI-NP – 3464),.

Deeba, F., Mirza, A.M., Mirza, N.M., 1999. Modeling and simulation of corrosion product activity in pressurized water reactors under power perturbations. Annals of Nuclear Energy 26 (7), 561–578.

Fontana, M.G., 1987. Corrosion Engineering, third ed. McGraw Hill, Singapore.

Glasstone, S., Sesonske, A., 1981. Nuclear Reactor Engineering. Von Nostradam, New York.

Hirschberg, G., Baradlai, P., Varga, K., Myburg, G., Schunk, J., Tilky, P., Stoddart, P., 1999. Accumulation of radioactive corrosion products on steel surfaces of VVER type nuclear reactors, Part I. 110 mAg. Journal of Nuclear Materials 265 (3), 273–284.

Iqbal, M., Mirza, N.M., Mirza, S.M., Ayazuddin, S.K., 1996. Study of the void coefficients of reactivity in a typical pool type research reactor (Volume Date 1997). Annals of Nuclear Energy 24 (3), 177–186.

Iqbal, M., Mirza, N.M., Mirza, S.M., 1998. Simulation of LEU-MTR transients under reactivity insertion and loss of flow conditions. Nuclear Science Journal 35 (2), 81–90.

Jaeger, R.G. (Ed.), 1970. Engineering Compendium on Radiation Shielding. Springer-Verlag, New York.

Kang, S., Sejvar, (1985, September). The CORA-II Model of PWR Corrosion Product Transport (EPRI - NP- 4246).

Khan, R., Mirza, N.M., Mirza, S.M., 1999. Ramp reactivity insertion limits in a typical pool-type research reactor. Nuclear Science Journal 36 (1), 27–41.

Lewis, E.E., 1977. Nuclear Power Reactor Safety. John Wiley, New York.

Mandler, J.W. et al., 1985. In-Plant Source Term Measurements at Praire Island Nuclear Generation Station (NUREG/CR-4397). US Nuclear Regulatory Commission.

Mirza, N.M., Mirza, A.M., Qaisrani, T.M., Ahmad, N., 1989. Effect of moderator temperature on dose rate due to Na-24 at the surface of a typical swimming pool research reactor. The Nucleus 26 (3), 23–28.

Mirza, N.M., Mirza, S.M., Ahmad, N., 1991. Study of coolant activation and dose rates with flow rate and power perturbations in pool-type research reactors. Nuclear Technology 96 (3), 237–247.

Mirza, N.M., Mirza, S.M., 1993a. Assessment of orifice effects on dose rates at the reactor bridge due to coolant activation in typical MNSRs. Nuclear Energy (Br. Nucl. Energy Soc.) 32 (6), 387–394.

Mirza, N.M., Mirza, S.M., 1993b. Effects of flow rate and power perturbations on dose rates due to coolant activity in low-power research reactors. Annals of Nuclear Energy 20 (6), 381–390.

Mirza, N.M., Chughatai, S.S., Ahmad, N., Khan, L.A., 1997a. Experimental measurements of sodium-24 activity in a typical low power tank-in-pool type research reactor. Nuclear Science Journal 34 (3), 203–208.

Mirza, A.M., Mirza, N.M., Mir, I., 1997b. Simulation of corrosion product activity in pressurized water reactors under flow rate transients. (Volume date 1998). Annals of Nuclear Energy 25 (6), 331–345.

Mirza, A.M., Khanam, S., Mirza, N.M., 1998. Simulation of reactivity transients in current MTRs. Annals of Nuclear Energy 25 (18), 1465–1484.

Nasir, R., Mirza, N.M., Mirza, S.M., 1999. Sensitivity of reactivity insertion limits with respect to safety parameters in a typical MTR. Annals of Nuclear Energy 26 (17), 1517–1535.

Polley, M.V., Anderson, P.O., 1989. Study of the integrity of radioisotope sampling from the primary coolant of Ringhals 3 PWR. Annals of Nuclear Energy 26 (17).

Raymond, A., De Murcia, A., Dhaunut, S., 1987. Speciation and analysis of corrosion products in the primary coolant of pressurized water reactors. Anal. Chim. Acta 195, 265–273.

Thomas, J.R., Edlund, H.C., 1980. Reactor Statics Module—Multi-group Criticality Calculations. Proc. Conf. ICTP, Trieste.

Varga, K., Hirchberg, G., Nemth, Z., Myburg, G., Schunk, J., Tilky, P., 2001. Accumulation of radioactive corrosion products on steel surfaces of VVER-type nuclear reactors. II. 60Co. Journal of Nuclear Materials 298 (3), 231–238.

Volleque, P.G., 1990. Measurements of radioiodine species in samples of pressurized water coolant. Nuclear Technology 90, 23–33.